Experimental Techniques for Measuring Temperature and Velocity Fields to Improve the Use and Validation of Building Heat Transfer Models

Brent T. Griffith **Daniel Türler** **Howdy Goudey** **Dariush K. Arasteh, P.E.**
Member ASHRAE

ABSTRACT

When modeling the thermal performance of building components and envelopes, researchers have traditionally relied on average surface heat-transfer coefficients that often do not accurately represent surface heat-transfer phenomena at any specific point on the component being evaluated. The authors have developed new experimental techniques that measure localized surface heat-flow phenomena resulting from convection. The data gathered using these new experimental procedures can be used to calculate local film coefficients and validate complex models of room and building envelope heat flows. These new techniques use a computer-controlled traversing system to measure both temperatures and air velocities in the boundary layer near the surface of a building component in conjunction with current methods that rely on infrared (IR) thermography to measure surface temperatures. Measured data gathered using these new experimental procedures are presented here for two specimens: (1) a calibrated transfer standard (CTS) that approximates a constant-heat-flux, flat plate; and (2) a dual-glazed, low-emittance (low-e), wood-frame window. The specimens were tested under steady-state heat flow conditions in laboratory thermal chambers. Air temperature and mean velocity data are presented with high spatial resolution (0.25 mm to 25 mm density). Local surface heat-transfer film coefficients are derived from the experimental data by means of a method that calculates heat flux using a linear equation for air temperature in the inner region of the boundary layer. Local values for convection surface heat-transfer rate vary from 1 W/m2·K to 4.5 W/m2·K. Data for air velocity show that convection in the warm-side thermal chamber is mixed forced/natural, but local velocity maximums occur from 4 mm to 8 mm from the window glazing.

INTRODUCTION

Nearly everyone has felt an uncomfortable draft standing near a window or sliding glass door during cold weather. Even if no outdoor air makes its way inside, natural convection produces a noticeable, downward flow of low-temperature air. This phenomenon has obvious implications—not only for thermal comfort of building occupants, it is also an important component of building envelope thermal performance, particularly for accurately determining surface temperatures or the likelihood of moisture condensation on the interior surfaces.

Current methods for analyzing building thermal performance use film coefficients to estimate surface heat-transfer rates. These coefficients are average values used to describe heat-transfer rates for the entire surfaces where the building envelope surface meets relatively still room air. Because these values are averages, they are often not accurate for specific locations on the surface. Although the growing use of computer simulations has allowed increasingly sophisticated analysis of the physical structure of building components, comparatively little improvement has been made in the analysis of surface heat-transfer phenomena. One way to improve the analysis of surface heat-transfer rates is to account for localized variations in both convective and radiative heat flows. The work described in this paper allows researchers to investigate localized convective heat flow.

Schrey et al. (1998) analyzed thermographic data for surface temperature and solved for local values of the convection portion of the film coefficient, h_c, for flush-mounted glazing units. In contrast to Schrey et al.'s research, which used an iterative approach that relied on computer simulations with film coefficient boundary conditions, we present techniques for gathering experimental data near an object's surface; these techniques may allow us to directly determine localized convective heat transfer coefficients, or local h_c.

Brent T. Griffith is a principal research associate, **Daniel Türler** is a senior research associate, **Howdy Goudey** is a senior research technician, and **Dariush Arasteh** is a staff scientist, Lawrence Berkeley National Laboratory, Berkeley, Calif.

Noncontact surface temperature measurements using infrared thermography have been used to validate simulations (Sullivan et al. 1996). However, one limitation of thermographic data for such purposes is that it gives only surface temperatures but not film coefficients at the time of the experimental measurements. Our current work is on developing expanded experimental techniques that allow measuring local convection effects during the testing of building assemblies in laboratory thermal chambers. These experimental techniques for mapping data for air temperature and velocity near the surface may be used to develop recommendations for localized values for natural convection. The data are also useful for validating conjugate CFD/heat-transfer simulations of building assemblies in laboratory chambers. Because laboratory thermal chambers use fans, one concern is whether the pure natural convection theory can be applied to predicting the performance of building assemblies tested in these chambers. Our experimental work may be used to test this assumption.

Two specimens were evaluated in the authors' infrared thermography laboratory: a calibrated transfer standard (CTS) and a wood-frame window with low-emittance (low-e) dual glazing. Data were collected for a vertical plane oriented perpendicular to the specimen at its center. Surface temperature data were gathered using infrared thermography. An automated traversing system was used to gather air temperature and velocity data. These high-resolution spatial data for temperature distributions are analyzed using fundamental equations from boundary-layer theory to predict local convection surface heat-transfer rates.

EXPERIMENTAL MEASUREMENTS

Laboratory experiments were conducted at the authors' laboratory. Figure 1 shows the configuration of the thermal chambers. Two laboratory environmental chambers were used to establish steady-state heat flow through the specimen in a fashion similar to that used in hot-box testing for winter heating conditions. However, the warm-side chamber where the measurements took place is designed for unobstructed access to the specimen and, therefore, does not employ a baffle in the way that a hot box does. The chambers and related instrumentation are described by Türler et al. (1997).

The cold-side chamber moves air up the back of the specimen in a plenum; velocity for these experiments was about 4.7 m/s at the middle of the specimen's main face during measurements. Bulk air temperature was measured at −17.8°C with a four-wire platinum resistance thermometer situated about halfway up the specimen. The mean surface heat-transfer coefficient on the cold side was measured at 33.4 $W/m^2 \cdot K$ using the CTS described below.

On the warm side of the specimen, air slowly circulates through a subfloor where the temperature is controlled. An air sink below the specimen removes cooled air. This temperature control scheme results in bulk air velocities of about 200 mm/s. Bulk air temperature was measured at 21.1°C with a four-wire platinum resistance thermometer situated at the top of the specimen, about 250 mm from the surface. The mean surface heat-transfer coefficient on the specimen's warm side was measured at 8.4 $W/m^2 \cdot K$ using the CTS described below. Although a desiccant system can be used to decrease the humidity in the warm chamber, it was not used for these experiments; the humidity level was about 45%.

Specimens Evaluated

We evaluated two specimens: a CTS and a wood-framed window with low-e dual glazing.

CTS. A CTS is a special thermal test assembly used to characterize mean surface heat-transfer coefficients in certain types of standardized hot-box testing (ASTM 1995).

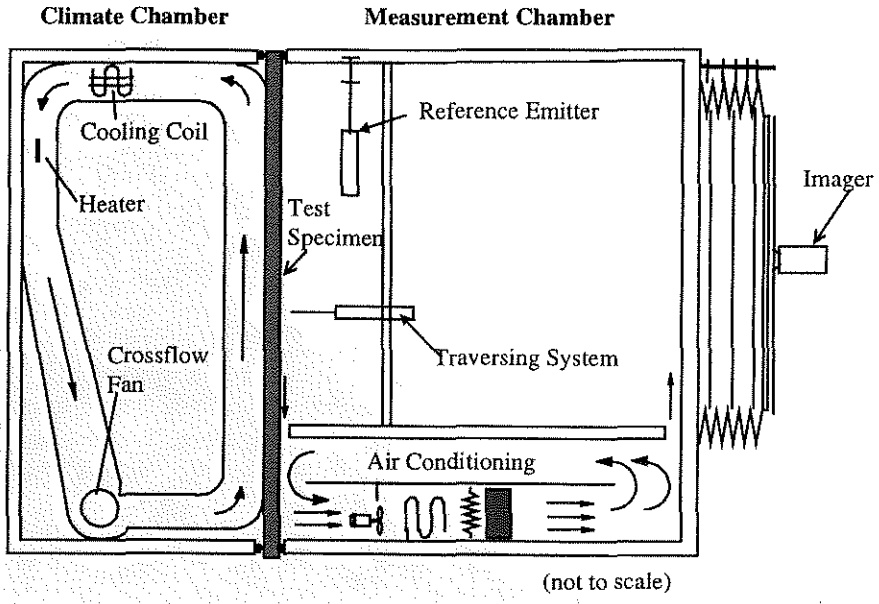

Figure 1 Laboratory chambers.

The CTS used for this experiment was constructed from expanded polystyrene foam board (EPS) that was 25.4 mm (1in.) thick and sandwiched between 4.7 mm (3/16 in.) glass sheets. The 912 mm (36 in.) square CTS has a total thickness of 35 mm (1 3/8 in.) and is mounted flush on its warm side in a 39.4 mm (1.5 in.) thick surrounding panel made of extruded expanded polystyrene foam (XEPS). Thermocouple arrays located at each interface between glass and EPS can be used to determine heat-flow rates, surface temperatures, and mean film coefficients.

Dual-Glazed Window. A wood casement window was obtained from a major manufacturer. The window was a fixed casement with a three-step frame profile. It had a low-e, dual-sealed, insulating glazing unit. The wood nailing flange and minor exterior trim sections were removed. Overall size was 916 mm (36 in.) high by 611 mm (24 in.) wide. Glazed area was 830 mm (32.7 in.) high by 525 mm (20.7 in.) wide. The window's frame profile, dimensions, and mounting for thermal testing are diagrammed in Figure 2. The window was mounted in a 117 mm (4.6 in.) thick XEPS surrounding panel that was approximately flush with the outer frame surfaces on both the cold and warm sides.

Traversing System Air Measurements

A computer-controlled motion system was used to move sensors in the air space near the specimens. This system collected air temperature and velocity data with high spatial resolution. Figure 3 depicts the traversing apparatus and shows the orientation of the plane (perpendicular to the specimen face) in which data were collected for this paper. The traversing system offers full control in three axes although the data presented here are only two-dimensional.

Because a specimen may not be perfectly flat and/or aligned to the traversing system, scanning the air space very near the surface requires a careful setup. Each specimen is first mounted in the thermal chambers and brought to steady-state conditions because it may bend or warp because of thermal expansion/contraction. The surface profile (specimen coordinate system) is characterized with respect to the traversing system's alignment (traversing system coordinate system) by sweeping an electronic dial gauge across the surface. (See Figure 5 for orientation of x and y coordinates.) The traversing system is then programmed to track the surface based on the dial gauge data, with resolution to 0.01 mm and estimated accuracy of 0.05 mm. The traversing program dictates the grid of measurement locations. In the x direction, the grid varies to provide higher resolution near interesting features such as the beginning of a flat specimen or the sill of a window. In the y direction, the data grid is varied to provide 0.25 mm resolution in the first 2 mm or 3 mm near the surface; resolution gradually decreases until the grid has 5 mm resolution at distances greater than 20 mm from the surface. As it tracks the surface, the traversing system corrects y locations at each x location so that the final data grid is orthogonal. A typical scanning experiment will measure 1,000 to 1,400 points in a grid that has

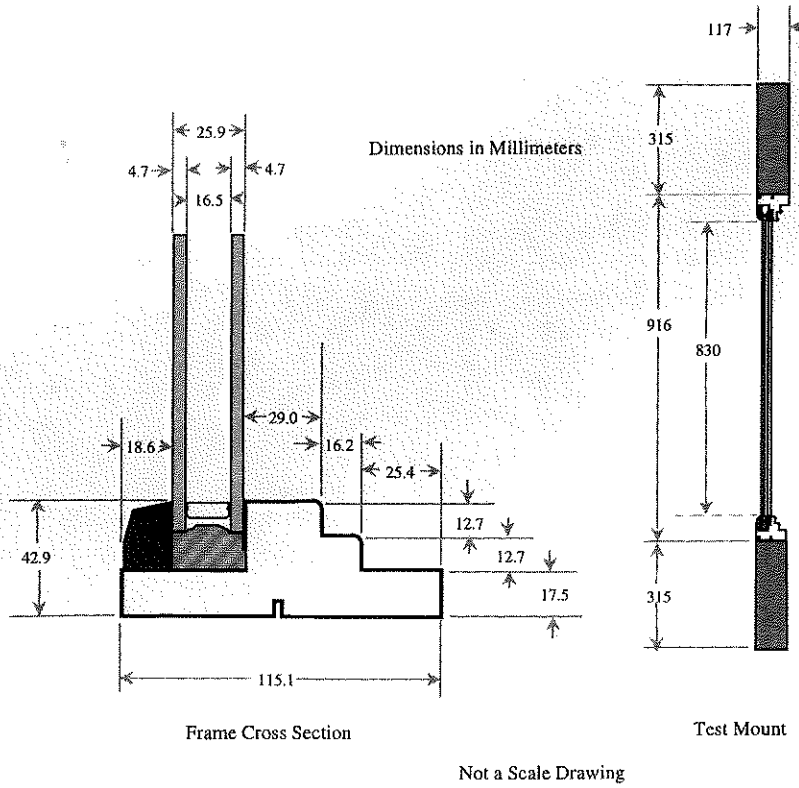

Figure 2 *Wood-frame window specimen and mounting.*

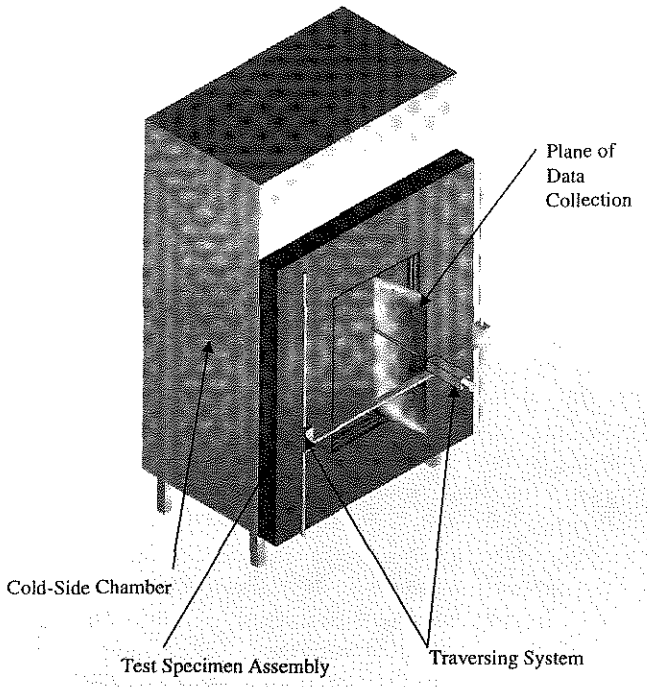

Figure 3 *Traversing system for air measurements, showing plane in which data are collected.*

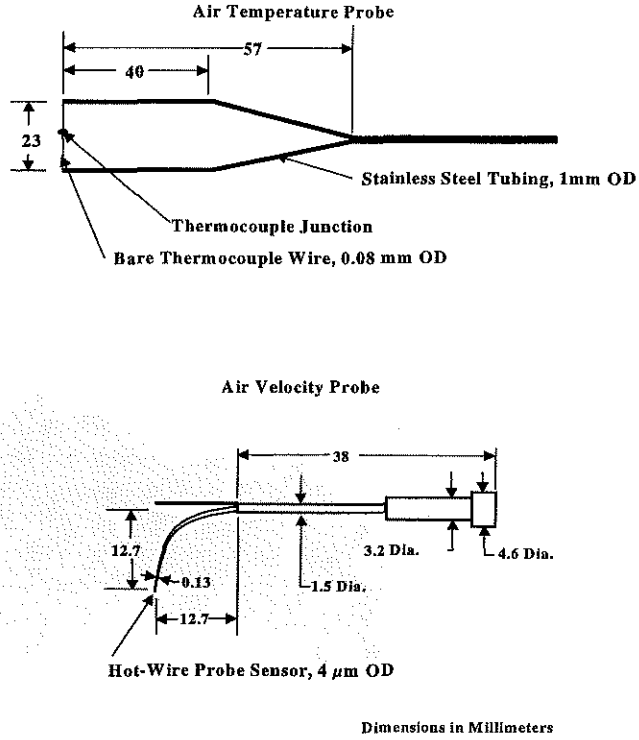

Figure 4 *Sensors used in traversing experiments.*

approximately 40 points in the x direction and 30 points in the y direction.

The traversing system rests at each grid point to gather a measurement before moving on to the next point. At the middle of the rest period, a trigger notifies the data-acquisition system to record values. Experiments presented here used a 40-second rest time with the data collected during a period of 20 seconds toward the end of the rest period. A typical scanning experiment ran for 10 to 15 hours, depending on the number of data points recorded.

Boundary-layer air temperatures were measured using a custom-built probe with a fine-wire, type-T thermocouple. The probe is diagrammed in Figure 4. The 40-gauge wire has a diameter of 0.08 mm (0.003 in.). The probe is read at 0.03°C resolution with an estimated accuracy of ± 0.3°C. The 16-bit data-acquisition system sampled the probe at 240 times per second and performed an initial average of every 40 values. These averaged data were then analyzed for a period of 20 seconds to determine the average value (variance of the data was also recorded). The probe and associated instrumentation were calibrated with a four-wire reference thermometer accurate to ±0.02°C by immersion in a temperature-controlled, stirred, fluid bath.

Air velocities were measured using a commercial, constant-temperature, hot-wire anemometer. The probe is diagrammed in Figure 4. The sensor wire has a diameter of 4 mm (0.00015 in.). Overheat level is about 100°C. The probe was calibrated for velocities from 0 mm/s to 400 mm/s using a sled technique in which the traversing system moves the probe through still air at a measured velocity. Resolution of the velocity measurements is 1 mm/s, but the precision is estimated at ±10 mm/s, and the bias in data could be as much as ±70 mm/s. The data-acquisition rates and analysis are the same as for the temperature probe.

Thermographic Surface-Temperature Measurements

Specimen surface temperatures were measured using infrared thermography and an external referencing technique. Detailed discussion of the equipment and techniques developed for this purpose are presented elsewhere (Griffith et al. 1995; Türler et al.1997; Griffith et al. 1998). The thermographic measurements presented here for the wood-frame window required more complicated procedures than needed for the flat specimen because the window frame surfaces were not flush. The complexities caused by self-viewing surfaces were accounted for by using small mirrors in a multistage process that gathered background radiation values for each surface. These procedures are discussed briefly in previous research (Griffith 1998). More research is needed on performing thermographic measurements of self-viewing surfaces, so the infrared data presented for the window specimen should be regarded as preliminary. External referencing of the infrared data used a target with a glass surface that was controlled by circulating water through a copper plate. Surface temperature data sets were generated with spatial resolution ranging from 1 mm to 3 mm temperature values have 0.1°C resolution and estimated accuracy of ±0.5°C.

POTENTIAL APPLICATIONS OF THE EXPERIMENTAL DATA

The temperature and velocity measurements made using the traversing system can be used to (1) calculate local convection coefficients for building assemblies and (2) validate computer models of building heat transfer and airflow.

Local Convection Coefficients

To make use of the detailed temperature maps gathered in these experiments so that we can calculate local convection film coefficients, we can analyze the gradients in the temperature distribution. This analysis is based on the classical heat-transfer boundary-layer analysis presented by Rohsenow and Choi (1961) and Raithby and Hollands (1975) A classic schematic used for visualizing natural convection down a cooled, vertical flat plate is shown in Figure 5. The wall has temperature T_s, and the air far from the wall has temperature T_∞. Because the wall is vertical, gravity (a body force), g_x, is oriented parallel to the wall. Direction y is away from the wall, and direction x is down the wall starting at the top of the specimen. The boundary layer next to a building component can be subdivided in two ways: the fluid boundary layer and the thermal boundary layer. The fluid boundary layer is characterized by a velocity profile; the thermal boundary layer is characterized by a temperature profile.

Fluid Boundary Layer. A thorough discussion of fluid boundary-layer theory is beyond the scope of this paper; our focus is on only one feature of this layer, referred to as the inner region. This is shown in Figure 5 as the region where $y < y_m$. The value of y_m corresponds to the distance from the wall where the air velocity has a local maximum as a result of natural convection. As the boundary layer develops or grows in the x direction, the value of y_m is expected to increase slightly. Note that at the surface of the wall, the velocity in both the x and y directions is zero. In the inner boundary layer region, there is no momentum transfer perpendicular to the wall, and viscous, buoyancy, and acceleration forces are balanced.

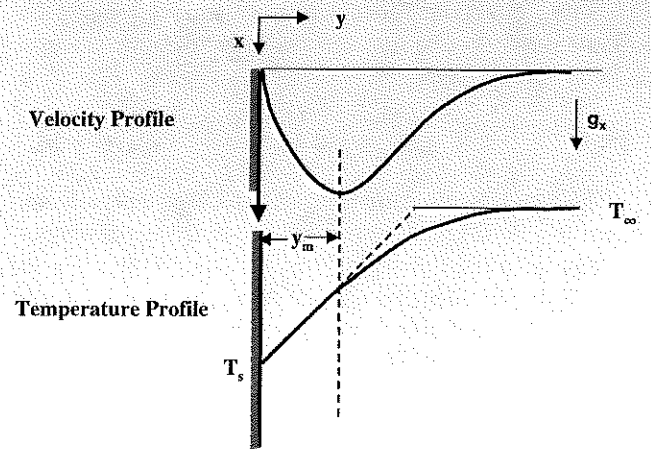

Figure 5 Boundary layer diagram.

Thus, the y component of velocity is zero in the inner region. We can then argue that there is no energy transport from mass transfer in this inner region. Therefore, the convective heat flow is purely from conduction within/across the inner boundary layer, which permits us to use Fourier's equation for heat conduction to characterize surface heat flows.

Identifying where the maximum velocity occurs should allow us to determine the extent of the inner boundary layer region in the y direction. This is shown in Figure 5 as the region $y < y_m$. If we are able to map the local air velocity maximum, we can be reasonably certain that we are within the inner boundary layer and, thus, that our temperature measurements were taken at a point between that maximum and the building component being analyzed (see Figure 5).

Thermal Boundary Layer. The analysis presented by Raithby and Hollands (1975) makes extensive use of a linear approximation for the temperature profile in the inner boundary layer region very near the surface of an object. This approximation is justified by and closely tied to the pure conduction mode of heat flow in the y direction in the inner boundary layer. Because the measurements presented in this paper have such fine resolution and are close to the surface, it is possible to analyze local convection using only the simple principle of pure conduction.

Thus, we make use of the following equations adapted from the literature (Rohsenow 1961) to determine values for natural convection. The temperature gradient in Equation 1 (DT/Dy) must be evaluated within the region where $y < y_m$.

$$Q_c = k\left(\frac{DT}{Dy}\right) \tag{1}$$

$$h_c = \frac{Q_c}{(T_\infty - T_s)} \tag{2}$$

where

Q_c = heat delivered to the surface by convection (W/m^2),
h_c = convection film coefficient (W/m^2·K),
k = thermal conductivity of still air (W/m^2·K),
T = air temperature (°C),
y = distance from plate (m),
T_∞ = air temperature (°C),
T_s = surface temperature (°C).

Data Analysis: Local h_c from Air Temperatures. Air-temperature data were collected at numerous x and y locations. The spatial coordinates for the temperature data were transformed into a flat coordinate system corresponding to the one shown in Figure 5. (When the surface was not flat to within 0.1 mm, we accounted for this in the traversing measurements; the data were transformed into a coordinate system that appears flat.) Data collected for air temperature were analyzed by fitting a linear equation for air temperature as a function of distance from the plate. For each x location, we fitted a line through eight points in the y direction within 3 mm from the

plate. The slope of this line became the value for *DT/Dy* at position *x*. The thermal conductivity of the air, *k*, is evaluated at the middle of the line (between the fourth and fifth data points—about 2 mm from the surface depending on the experiment) by interpolating between two literature values for *k*, 0.02408 W/m^2·K at 0°C and 0.02614 W/m^2·K at 26.85°C (Liley 1968). Surface-temperature data were gathered using infrared thermography with a high spatial resolution of about 1 mm, and a fifth-order polynomial equation curve fit was used to convert the data for T_s between coordinate systems. The CTS also has direct contact sensors embedded in it, which provides six temperature points along the middle of the specimen; these data were also fit with a fifth-order polynomial equation to provide a second set of values for T_s for the CTS.

Applications for Model Validation

The data gathered by the traversing system can also be used to validate sophisticated computer simulation tools that are used to analyze energy use and comfort in buildings. Two general types of simulation programs that are used focus on the details of heat flow through components of a building's thermal envelope and those that focus on the details of airflow inside a building's occupied spaces. The first type of program simulates heat transfer by conduction in two or three dimensions using thermal models that extend between the interior and the exterior surfaces of the building thermal envelope. These programs can be used to generate ratings for fenestration products and are beginning to incorporate modeling of localized surface heat-transfer effects by means of improved radiation modeling algorithms and variable boundary condition inputs (Arasteh et al. 1998a). The second type of computer program used to analyze buildings relies on computational fluid dynamics (CFD) solution techniques to simulate airflows in occupied spaces inside a building's thermal envelope (Chen 1997; Ladiende and Nearon 1997). CFD programs can predict the energy use and thermal comfort of complicated building spaces such as glazed atria (Schild 1996).

Building heat-transfer and CFD simulations are sometimes merged together in sophisticated conjugate simulations that predict both heat and fluid flows (Chen et al. 1995). Conjugate simulations can account for localized radiation and convection effects although they are not often solved because of the considerable computational effort that is required to model fluid motion.

Both types of simulation programs make predictions that are affected by surface heat-transfer phenomena and could benefit from being able to use local values for film coefficients. For example, Griffith et al. (1998) and Arasteh et al. (1998b) showed that element-to-element radiation view-factor modeling improves the accuracy of surface temperature results for projecting fenestration products. This research also identified complicated convection phenomena as the cause of differences between the experimental and simulated data. Accounting for local radiation and convection effects would be especially useful for rating product performance for condensation resistance. Proposed voluntary Canadian fenestration standards suggest varying the convection coefficient by stepped amounts when simulating the condensation performance of the bottom edge of a window (Glover 1998). While this procedure is definitely an improvement over the use of a constant film coefficient, basing such modeling guidelines on experimental results would improve their validity.

Computer simulations are often validated by comparison to experimental measurements. Heat-transfer simulations of building assemblies are usually compared to U-factors measured under steady-state conditions in laboratory thermal chambers (Elmahdy 1992). Though some detailed experimental data are available for room airflows (Murakumi et al.1994), it is common to verify CFD simulations in a two-step process that first compares results for a standard benchmark case and then applies the simulation algorithms to the desired model (Curcija 1992).

Using a modern, computer-controlled traversing system to gather large sets of data with fine spatial resolution offers a new way to test the accuracy of simulated data. Instead of extracting small parts of the temperature or flow field, entire matrices of data could be compared. Specimens with complicated surface geometry can also be evaluated, providing more rigorous testing of a model than is possible with classic flat-plate solutions.

RESULTS

The traversing system was used to test two specimens. Chamber operation over the approximate 12-hour time period of the experiments was fairly stable, with temperatures controlled to within ±0.1°C. Uncertainty in the traversed air temperature measurements is estimated at ±0.3°C. Uncertainty in the thermographic surface temperature measurements is estimated at ±0.6°C. Bias error in the velocity measurements could be as high as 100 mm/s, but the velocity data are estimated to be precise to within ± 10 mm/s. Uncertainty in position is estimated at ±0.2 mm in the *y* direction and ±0.4 in the *x* direction. The traversing system setup found that the glass surfaces of both specimens deflected by distances of about 0.5 mm to 1 mm.

CTS

The experiments using the CTS focused on gathering temperature data. Figure 6 shows the complete set of temperature data including the air temperatures near the surface of the CTS and the surface temperatures determined from infrared thermography. Figure 7 shows selected air temperature profiles very near the CTS and linear curve fits of the type that could be used to generate local convection film coefficients. Figure 8 shows the results for local convection coefficients obtained by analyzing the temperature gradient in the air within 3 mm of the CTS surface.

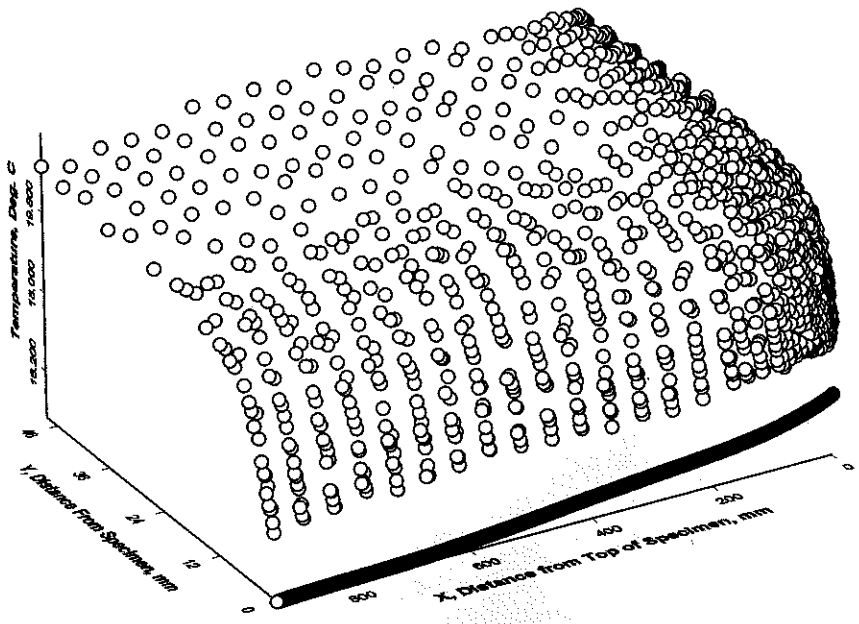

Figure 6 *CTS temperature map: air temperatures and infrared surface temperatures.*

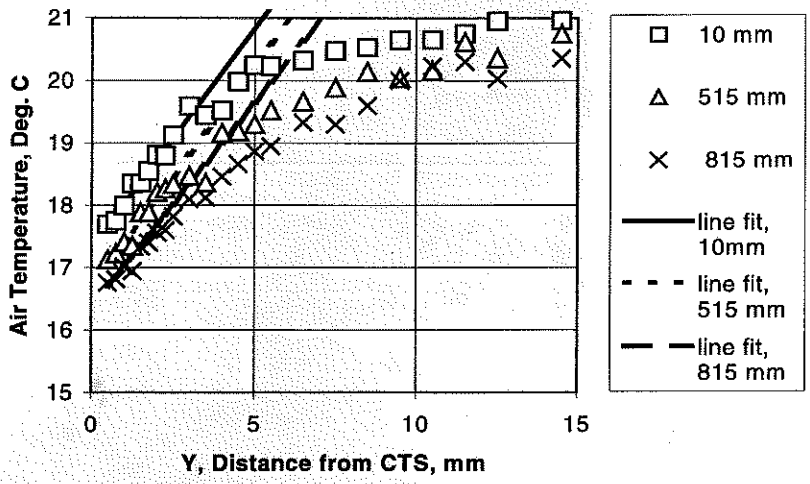

Figure 7 *Air temperature profiles near the CTS at three locations, showing linear fits used for local convection coefficients.*

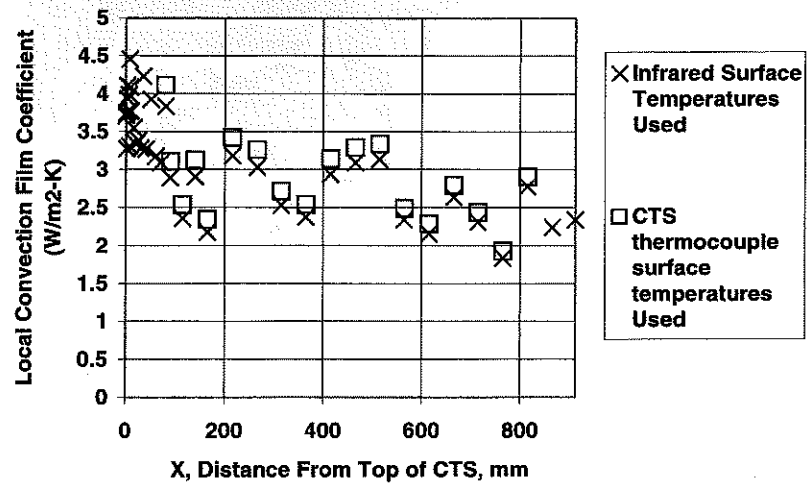

Figure 8 *Local convection coefficients along the CTS from the top down, as analyzed from air temperature gradients.*

Window

Both air temperature and velocity data were gathered for the wood-frame window with low-e glazing focusing on the glazing portion of the specimen. For the traversing experiments, humidity was not suppressed and condensation was present on the lower 100 mm (x = 730 to 830) of the glazing at the sill. The air dryer was used, however, during the thermographic measurements. Figure 9 shows the complete set of temperature data including the air temperatures near the surface of the window glazing and the surface temperatures determined from infrared thermography. Figure 10 shows the complete set of air velocity data near the surface of the glazing. Figure 11 shows selected horizontal velocity profiles at three distances from the top of the glazing. Figure 12 shows selected vertical velocity profiles at three different distances down the glazing. Figure 13 shows the results for local convection coefficients obtained by analyzing the temperature gradient in the air within 3 mm of the specimen's surface.

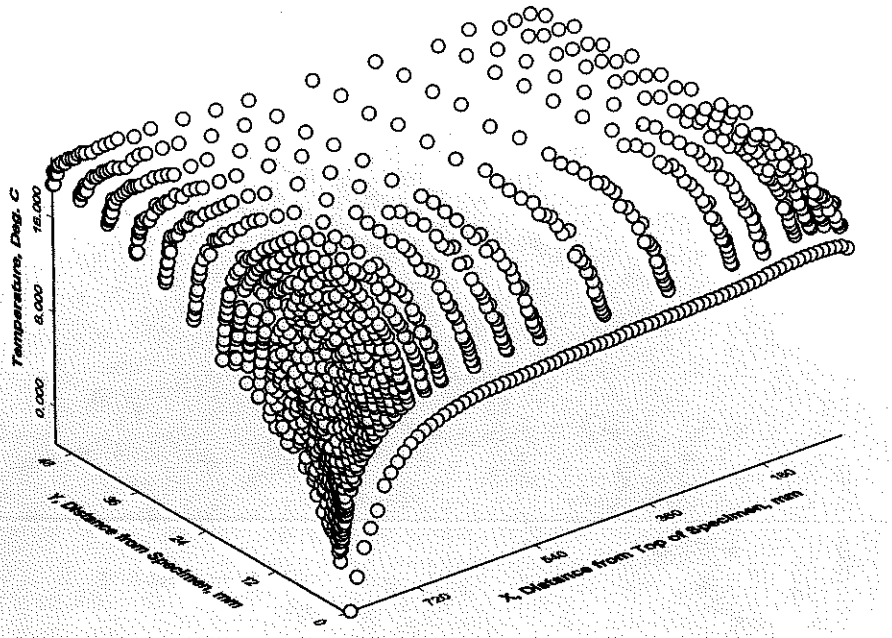

Figure 9 *Wood window glazing temperature map: air temperatures and infrared surface temperatures.*

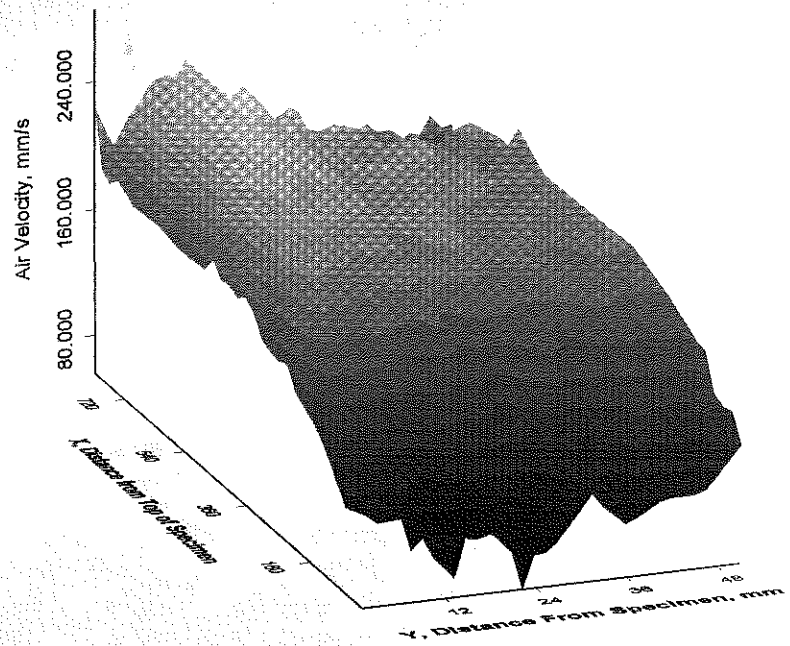

Figure 10 *Wood window glazing, air velocity measurements.*

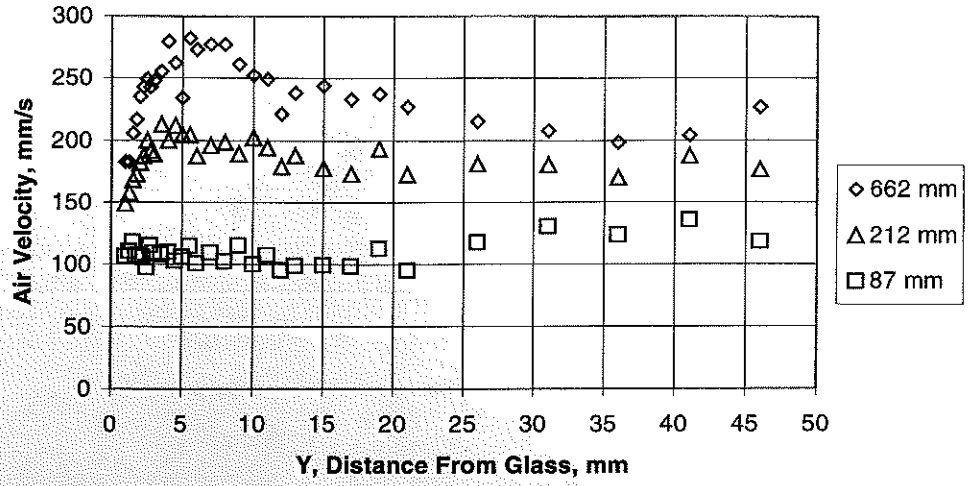

Figure 11 Selected horizontal profiles of air velocity near window glazing at three distances from the top of the glazing.

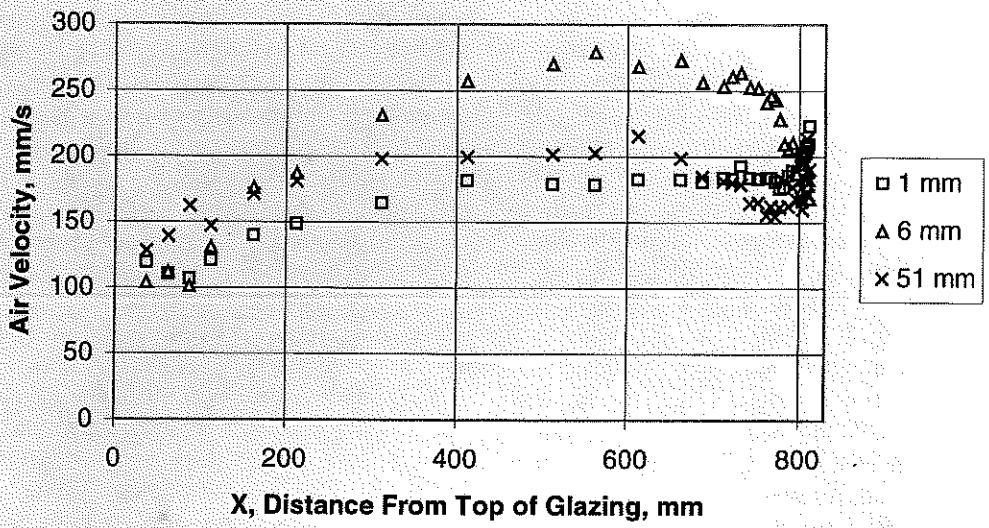

Figure 12 Selected vertical profiles of air velocity near window glazing at three distances away from the glass.

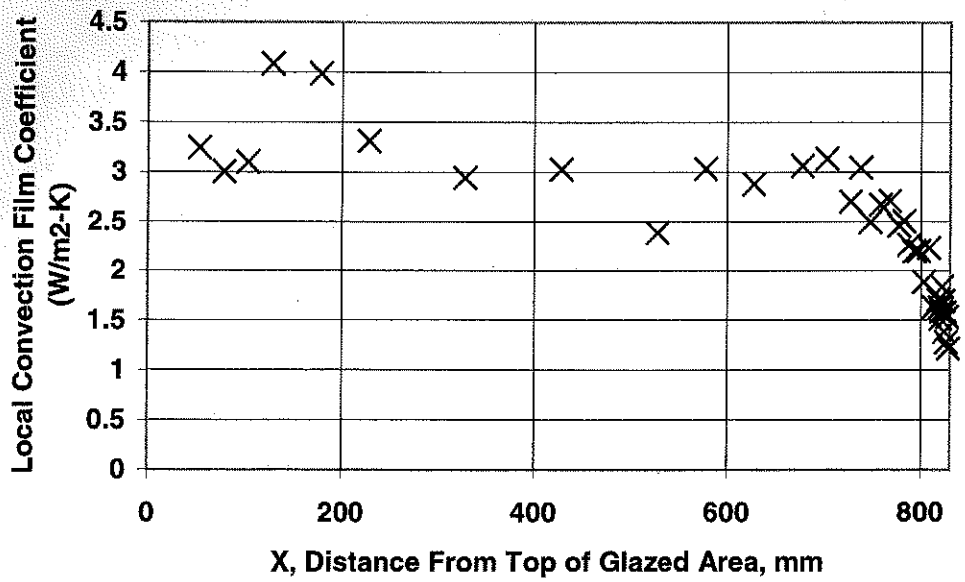

Figure 13 Local convection coefficients along window glazing from the top down as analyzed from air-temperature gradients.

DISCUSSION

Mapping with high spatial resolution the air conditions near a thermal test specimen is a feasible technique for researching localized heat transfer phenomena. The large sets of data for temperature and velocity that can be gathered with a computer-controlled traversing and data acquisition system should prove useful for improving the analysis of building thermal envelope heat flows. The combination of data for both thermal and fluid phenomena measured by the traversing system is useful for validating steady-state, conjugate CFD simulations. Researchers interested in obtaining our results are encouraged to contact the authors for electronic versions of data sets (see http://windows.lbl.gov).

Our temperature-distribution results show that air temperature can be considered linear in the inner region of the thermal boundary layer, as theory leads us to expect. The velocity profiles for the window show that, although the flow is not purely natural convection, there is a local velocity maximum that occurs as would be expected for pure natural convection. This maximum was found to occur from 4 mm to 8 mm from the surface of the window (4 mm $< y_m <$ 8 mm), indicating that $y <$ 3 mm is safely inside an inner boundary layer region. Thus, it appears that although the fan mixing of air in the thermal chamber results in mixed forced and natural convection, local convection dominates sufficiently to allow determining local convection coefficients by analyzing the temperature gradients in air and assuming pure conduction in this region.

The temperature gradients near the surface were analyzed to determine local surface heat-transfer coefficients resulting from convection. The values obtained for local convection coefficients appear to be reasonable, displaying the trends and magnitudes that are in accordance with theory. However, there is currently no independent method of verifying that the results are accurate. More testing of the procedure for determining local coefficients is needed.

FUTURE RESEARCH

The techniques presented in this paper will continue to be used as part of research efforts to develop both improved inputs for use in performing building simulations (e.g., local film coefficients) and an improved method for verifying the accuracy of simulated results. Subjects recommended for future study using these techniques are listed below.

1. *Performing isothermal flat plate measurements.* Measuring conditions near an isothermal flat plate in laboratory thermal chambers could provide a good opportunity to evaluate how well engineering theory can be applied to the problem of predicting the performance levels of building assemblies in a hot box test.
2. *Determining local coefficients from temperature boundary-condition modeling.* An independent method of determining local convection coefficients is being developed that uses thermographic data as modeling inputs.
3. *Performing three-dimensional measurements.* Software to control the traversing system is being developed to simplify setup and enable collection of data resolved in three dimensions.
4. *Characterizing turbulence intensity.* Data collection routines are being refined to allow characterization of the velocity and temperature variations over time.
5. *Investigating air humidity interactions.* Brandli et al. (1996) identified that radiation absorption by moisture in the air can produce a measurable effect on the temperature profile and thus affect convective film coefficients. This phenomenon will be investigated.

CONCLUSIONS

The steady-state, thermal testing of building assemblies can be augmented by measuring with high spatial resolution temperatures and velocities using a traversing system. Data can be obtained within the thermal boundary in detail sufficient for determining local film coefficients that could be used to improve the boundary-condition inputs in heat transfer models. The computer-controlled, motion/data-acquisition system allows collection of large and complicated data sets that could be used to check the accuracy of sophisticated computer simulations of conjugate problems of heat transfer and fluid dynamics in buildings.

ACKNOWLEDGMENTS

The authors thank Nan Wishner for her assistance in editing this paper. This work was supported by the Assistant Secretary for Energy Efficiency and Renewable Energy, Office of Building Technology, State and Community Programs, Office of Building Systems of the U.S. Department of Energy under Contract No. DE-AC03-76SF00098.

REFERENCES

Arasteh, D., E. Finlayson, R. Mitchell, C. Huizenga, and D. Curjica. 1998a. THERM 2.0: Program description. LBL Report 37371. Berkeley, CA.

Arasteh, D., E. Finlayson, D. Curjica, J. Baker, and C. Huizenga. 1998b. Guidelines for modeling projecting fenestration products. *ASHRAE Transactions* 104(1B): 856-860.

ASTM C 1199. 1995. Standard test method for measuring the steady-state thermal transmittance of fenestration systems using hot box methods. *1995 Annual Book of ASTM Standards*, Vol. 04.06, pp. 658-669. American Society for Testing and Materials.

Brandli, M., G. Schenker, and B. Keller. 1996. The interaction of the infrared radiation from the room boundaries with the humidity content of the enclosed air. *5th International conferences on Air Distribution in Rooms, ROOMVENT'96.* July 17-19.

Chen, Q. 1997. Computational fluid dynamics for HVAC: successes and failures. *ASHRAE Transactions* 103(1): 178-187.

Chen, Q., X. Peng, and A.H.C. van Paassen. 1995. Prediction of room thermal response by CFD technique with conjugate heat transfer and radiation models. *ASHRAE Transactions* 101(2): 50-60.

Curcija, D. 1992. Three dimensional finite element model of overall nighttime heat transfer through fenestration systems. Ph.D dissertation, University of Massachusetts, Amherst.

Elmahdy, A.H. 1992. Testing and simulation of high-performance windows—Phase II of the Canadian/U.S. joint research project on window performance. *Thermal Performance of the Exterior Envelopes of Buildings V.* Atlanta: American Society of Heating, Refrigerating and Air-Conditioning Engineers, Inc.

Glover, M. 1998. Proposed Change to CSA Standard A440 Condensation Resistance Test, January 11.

Griffith, B.T., F. Beck, D. Arasteh, and D. Turler. 1995. Issues associated with the use of infrared thermography for experimental testing of insulated systems. *Thermal Performance of the Exterior Envelopes of Buildings VI.* Atlanta: American Society of Heating, Refrigerating and Air-Conditioning Engineers, Inc.

Griffith, B.T., D. Curcija, D. Turler, and D. Arasteh. 1998. Improving computer simulations of heat transfer for projecting fenestration products: Using radiation view-factor models. *ASHRAE Transactions* 104(1B): 845-855.

Ladeinde, F., and M.D. Nearon. 1997. CFD Applications in the HVAC&R industry. *ASHRAE Journal*, January.

Liley, P.E. 1968. The thermal conductivity of 46 gases at atmospheric pressure. *Proceedings of the Fourth Symposium on Thermophysical Properties.* College Park, Md.:American Society of Mechanical Engineers.

Murakami, S., H. Yoshino, S. Kato, T. Harada, and T. Hiramatsu. 1994. Sample data for testing models of air and temperature prediction in large enclosures—Time dependent data of experimental atrium. Institute of Industrial Science, University of Tokyo, Japan.

Raithby, G.D., and K.G.T. Hollands. 1975. A general method of obtaining approximate solutions of laminar and turbulent free convection problems. *Advances in Heat Transfer*, 11:265-315. Academic Press.

Rohsenow, W.M., and H.Y. Choi. 1961. *Heat, mass, and momentum transfer.* Englewood Cliffs, N.J.: Prentice-Hall.

Schild, P.G. 1996. CFD analysis of an atrium, using a conjugate heat transfer model incorporating long-wave and solar radiation. *5th International Conference on Air Distribution in Rooms, ROOMVENT'96.* July 17-19.

Schrey, A., R.A. Fraser, and P.F. de Abreu. 1998. Local heat transfer coefficients for a flush-mounted glazing unit. *ASHRAE Transactions* 104(1B):1207-1221.

Sullivan, H.F., J.L. Wright, and R.A. Fraser. 1996. Overview of a project to determine the surface temperature of insulated glazing units: Thermographic measurements and two-dimensional simulations. *ASHRAE Transactions* 102(2): 516-522.

Türler, D., B. Griffith, and D. Arasteh. 1997. Laboratory procedures for using infrared thermography to validate heat transfer models. *Insulation Materials: Testing and Applications*: Third Volume ASTM STP 1320. R.S. Graves and R.R. Zarr, eds. Philadelphia, Pa.: American Society for Testing and Materials.